Assembly and test runs of decay detector for ISGMR study

J. Button, R. Polis, C. Canahui, Krishichayan, Y. -W. Lui, and D. H. Youngblood

1. ΔE- ΔE - E Plastic Scintillator Array Decay Detector

In order to study the Isoscalar Giant Monopole Resonance in unstable nuclei, we have designed and built and are testing a ΔE- ΔE - E decay detector composed of plastic scintillator arrays. The elements of this detector and its paramters are descirbed in Ref. [1].

Currently, the decay detector is nearly completed. A new set of 12 horizontally aligned and 14 vertically aligned scintillator strips have been prepared for installation. The original design for holding vertical scintillator strips has been found to be unsuitable and is still being re-worked. Testing has been done to eliminate detector elements or identify elements in need of modification (scintillator strips and blocks, photomultiplier tubes, optical fibers, or light windows).

2. Calculating Light Output

Two methods for the calculation of relative light output of plastic scintillator when ions of a particular energy pass through or are stopped in the scintillator will be compared for suitability in calibrating light output from the experimental setup. An empirical relationship such as the Birks formula[2], which relates light output to the stopping power directly, is a convenient method because of the widespread availablity of stopping power tables for energetic ions passing through matter[3]. Also, the stopping power may be calculated directly by the Bethe-Bloch formula [5]. The Birks formula becomes a hindrance when the experiment involves many ion types, since the parameters L_0 and K will vary by ion type. For this situation, models with a specific Z dependence have been proposed. One such model (Energy Deposition by Secondary Electrons) relates light output $\frac{dL}{dx}$ to the number of energy carriers (electron-hole pairs or excited molecular structures) created due to energy loss of the ion in the scintillating material [6]. Non-linearities in the light response originates when the energy carrier density exceeds the quenching density, ρ_q. The number of energy carriers, $\frac{dN_e}{dx}$, is obtained via radial integration of the energy carrier density $\rho(r)$, where x is the ion path through the scintillating material and r is a distance perpendicular to x indicating the path of energy carriers through the material. For plastic scintillators like BC408, the specific detector response, $\frac{dL}{dx}$, is related to the number of energy carriers by equation 1.

$$\frac{dL}{dx} = C\frac{dN_e}{dx}\left(1 - F\frac{dN_e/dx}{A + dN_e/dx}\right) \quad (1)$$

The fit parameters C, F, A and ρ_q were obtained by fitting to published experimental data where the ion is stopped in the scintillator [4] (Fig. 1). These parameters were then used to obtain the expected light

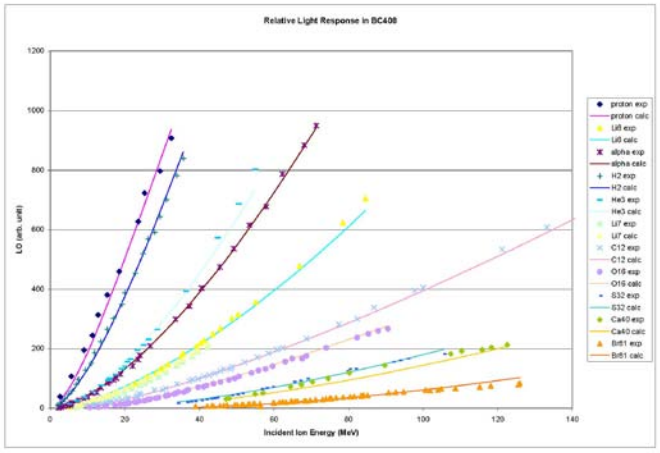

FIG. 1. Comparison of EDSE model to experiment [4] for various ions, where the ion is stopped in the material. The fit parameters are C = 11.51, A = 266.38, F = .882, ρ_q =1.83*10^{26}.

response due to protons or alpha ions that only deposit a small portion of their energy in 1 mm thick strip scintillators (Fig. 2).

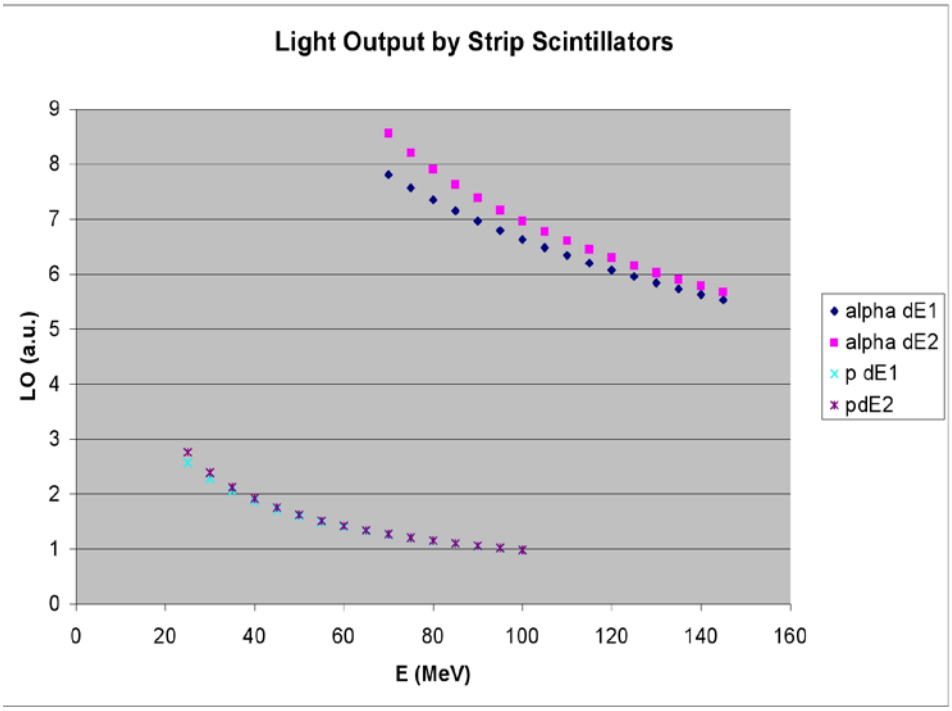

FIG. 2. Calculation of light output in ΔE1 and ΔE2 for protons and alpha ions.

3. ^{90}Sr Beta Source Testing

The light output response by a 1 cm diameter cylindrical BC408 plastic scintillator due to ^{90}Sr beta electrons was measured. This cylindrical scintillator was then used to compare performance between all 1 cm diameter photomultiplier tubes. A scintillator of this thickness is sufficient for stopping all electrons produced in the decay of $^{90}\text{Sr} \rightarrow {}^{90}\text{Y} + \beta^-$ (Q value of 546 keV). The ^{90}Y undergoes a subsequent beta decay (Q value of 2.4 MeV). The signal from the photomultiplier tube was passed through a spectrum amplifier, sent to a multichannel analyzer, and recorded by computer.

To calibrate the measured spectrum to the known energy spectrum, one can make a Fermi-Kurie plot (Fig. 3) [8]. When this transformation is applied, the tail part of the energy cross-section is linear with respect to the electron energy (Eq. 2), making it very simple to find the end point of the spectrum (~ 2.4 MeV). At this energy scale, the relationship between light response by the plastic scintillator and the energy deposited into the scintillator by the beta electron is linear. The response by the photomultiplier tube, the spectrum amplifier, and the multichannel analyzer are each assumed to be linear as well.

$$\sqrt{\frac{dN(p_{e^-})/dE}{p_{e^-}^2 F(Z_D, p_{e^-})}} \propto (E - E_{e^-})\left|M_{fi}\right| \qquad (2)$$

p_{e^-} is electron momentum, $F(Z_D, p_{e^-})$ is the Fermi Function, and $\left|M_{fi}\right|$ is the transition matrix element.

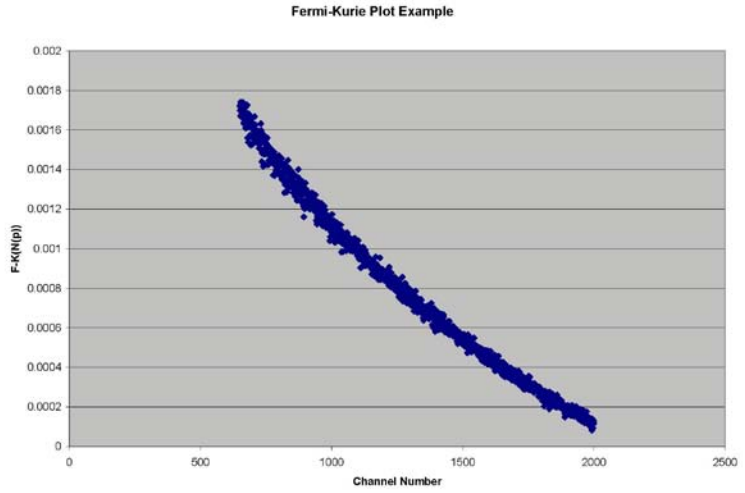

FIG. 3. Example of a Fermi-Kurie plot.

The normalized spectrum measured by each photomultiplier tube was graded against the average response from all photomultiplier tubes (Fig. 4). The gain with the same voltage applied differed by as much as 100%. A set of tubes whose gains agreed to 15% were chosen for the detctor.

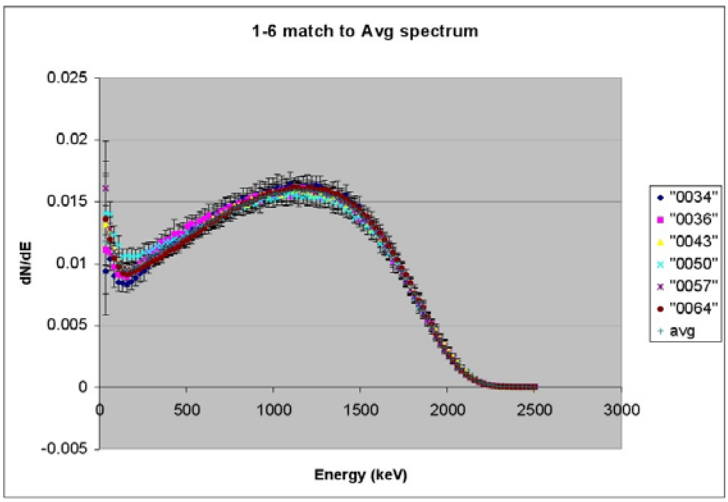

FIG. 4. Normalized and calibrated spectra from separate photomultiplier tubes and the average spectrum from all tubes. The observed peaks are from the beta decay of ^{90}Y.

4. Modifications to Detector Design and Assembly

In order to make and secure the joint between the scintillator and the optic fiber bundle, a thin, plastic sleeve was made to fit over the joint. The sleeve ensures proper alignment between the scintillator and fiber bundle over the course of the optical cement curing time (~24 hours) (Fig. 5)

FIG. 5. Optic Fiber Bundle enclosed by thin strips of plastic: open cavity is filled with optical cement and thin strip scintillator in order to make a secure and rigid joint.

Scintillator strips are held onto their alignment frame at two points: at the sleeve joint by an aluminum clamp which can be screwed into place on the frame and at the end of the scintillator strip by a

small neodymium magnet (Fig. 6). The strips at 0^o, however, are only half the length as all other strips and are only supported at the sandwich joint. In the future, the brass collimator at 0^o will be modified so that these strips may also be held in place at their ends.

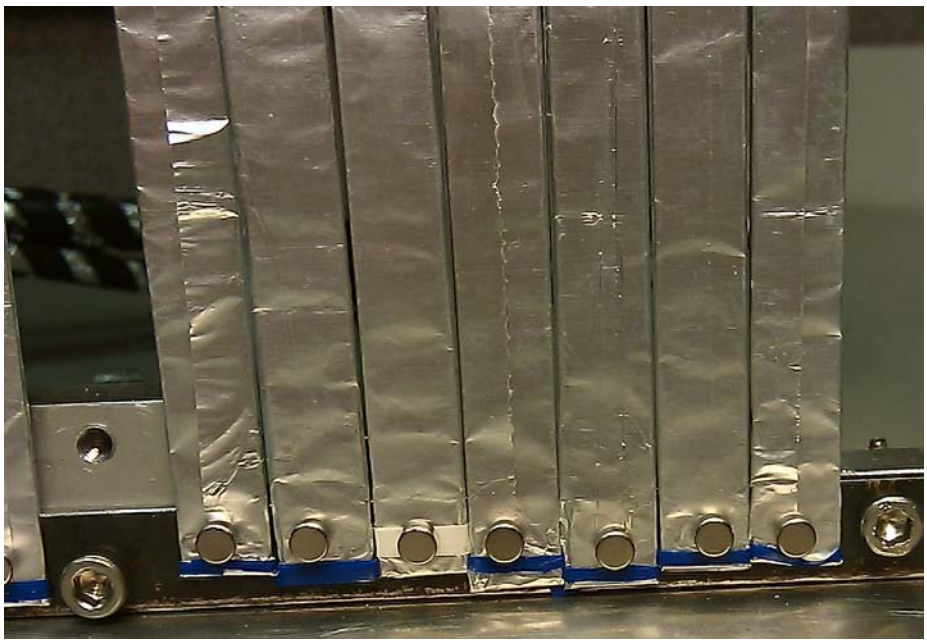

FIG. 6. Magnets used to hold vertical scintillator strips

In prior test runs, the optical cement joints between the block scintillators and their odd-shaped light-guides and between the odd-shaped light-guides and cylindrical light-guides were prone to breaking upon installation into a plate which is mounted onto the top of the target chamber lid. A holder supports each block separately by an o-ring which goes around the cylindrical light-guide and an aluminum clamp with a crush gland machined into it which bolts onto the plate (Fig. 7), which has five holes at positions

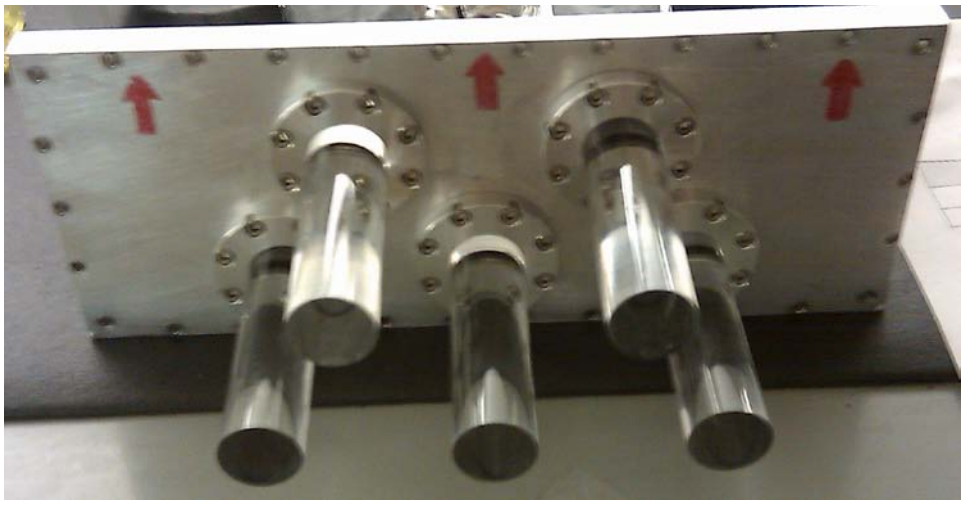

FIG. 7. Plate and Holders support each block scintillator and its light guides.

corresponding to the position of the five block scintillators. In order to prevent breaking, great care must be taken in making the optical cement joints. Proper alignment can be acheived by sandwiching the joint between a scintillator and its light guide with four blocks of plywood (Fig. 8). Wax paper is sufficient to prevent cementing the scintillator or light-guide to the plywood. After this joint has been made for each of the blocks, the blocks are then bundled together and held in a box (Fig. 9). The cylindrical light guides are clamped by each holder onto the plate. Dowel pins along the edge of the box are used to align the plate onto the top of the box, ensuring that the cylindrical light-guides are properly aligned with their corresponding odd-shaped light-guides.

FIG. 8. Making the joint between a block scintillator and its light-guide.

FIG. 9. Box used for aligning cylindrical light-guides to odd-shaped light-guides.

5. Test Run and Analysis

For the June 2010 test run, the decay detector consisted of 3 block scintillators, 15 vertical scintillators, and 12 horizontal scintillators. Data were taken using beams of 100 MeV α particles and 30 MeV protons on ^{12}C and ^{58}Ni targets. During this test, much time was dedicated to identifying components that were not working properly. With the exception of one signal from a horizontal strip, all scintillator strip signals were taken without amplification. The horizontal layer of strips was used as a trigger. All triggered events were recorded. Only those events having a coincidence between the horizontal and vertical arrays were analyzed.

Ratios of elastic peak position (LO(α)/LO(p)) in the individual spectra of various strip

scintillators were calculated and compared to measurement in Table I. Some strips had poor agreement with calculation, and this was determined to be due to poor optical connections between fiber bundle and scintillator. Insufficient gain from the electronics may have also been a significant factor.

Table I. Comparison of 100 MeV α and 30 MeV proton elastic peaks at various angles through 1 mm thick BC408 plastic scintillator. EDSE model is used to arrive at the calculated ratio of alpha to proton peak positions.

	est. angle (deg.)	energy_α (MeV)	energy_p (MeV)	LO(α)/LO(p) calc.	LO(α)/LO(p) exp	% diff calc. to exp.	dE_α (MeV)	dE_p (MeV)
v9	5.5	99.7	30.0	2.9	2.9	-1.4%	9.0	1.9
v12	21.2	95.5	26.7	2.7	2.6	3.9%	9.4	2.1
v14	30.2	91.2	29.3	2.9	2.4	20.5%	9.7	2.0
h1	37.5	86.8	29.0	3.0	3.9	-23.2%	10.1	2.0
h3	29.9	91.3	29.3	2.9	2.8	5.9%	9.5	2.0
h4	25.9	93.4	29.5	2.9	2.2	33.9%	9.3	2.0
h5	21.2	95.5	29.7	2.9	2.1	37.7%	9.2	2.0
h6	16.2	97.4	29.8	2.9	2.1	35.1%	9.1	1.9
h7	11.0	98.8	29.9	2.9	2.9	-2.1%	9.0	1.9
h9L	0.0	100.0	30.0	2.8	2.6	10.5%	9.0	1.9
h10	5.5	99.7	30.0	2.8	2.8	0.8%	9.1	1.9
h11	11.0	98.8	29.9	2.9	2.0	40.1%	9.2	2.0
h9R	0.0	100.0	30.0	2.8	3.2	-11.3%	9.0	1.9

Another test run was done in December 2010 with 30 MeV protons incident on targets of ^{12}C and ^{58}Ni. Analysis on data collected at this time focused on the attenuation of the light response by the thin, strip scintillators for charged ions incident upon a scintillator at different positions relative to the optical connection with the fiber bundle. This was examined in detail using horizontal strip H3 because it was the newest strip installed into the array and had the best light response of all scintillator strips. Spectra obtained from H3 in coincidence with the 5 E blocks were considered only because the E blocks showed better uniformity in terms of response from block to block. Taking into consideration the wrapping used (a layer of aluminum foil) and the position of H3, the energy of elastically scattered protons off of a target of ^{12}C should range from 28.8 MeV to 29.1 MeV, only a spread of 1%. In Figure 10 however, the spread of the light response along the length of H3 is nearly 53%. The effective length of H3 was taken to be 14.2 cm since that is the width of the E block array and because only events in coincidence with the E block array were considered. The positions of the elastic peak in each of the 5 spectra were measured (Fig. 10). The expected positions of the elastic peak in each spectrum are shown in Figure 11 The measured peak positions were then corrected by the expected change in light response and then plotted against position along strip H3. Even though the expected change is very small, it was assumed that this method would give a more precise estimate of the attenuation length, which was found to be 12.1 +/- 4.5 cm (Fig. 12).

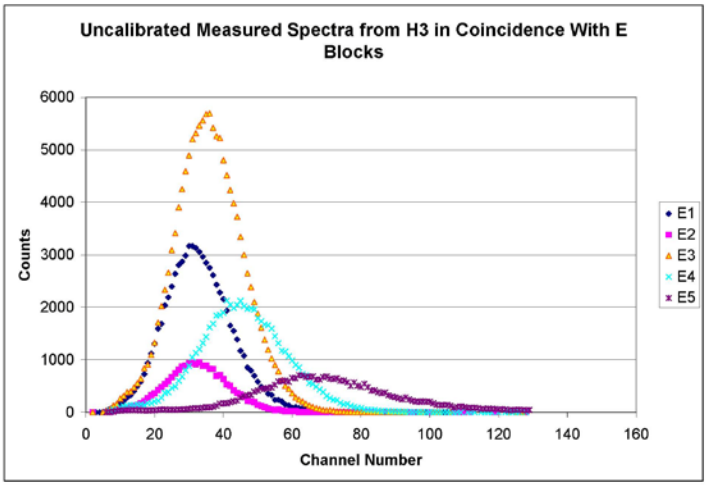

FIG. 10. 30MeV proton on 12C; raw spectra from scintillator strip H3 in coincidence with the 5 E blocks.

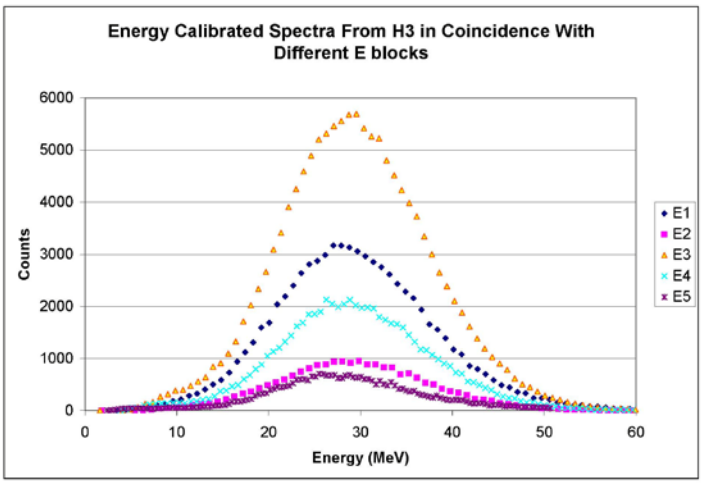

FIG. 11. 30MeV proton on 12C; calibrated spectra from scintillator strip H3 in coincidence with the 5 E blocks.

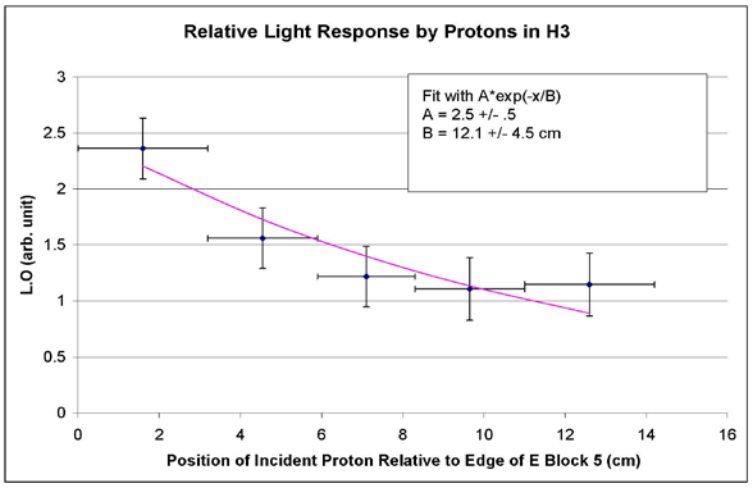

FIG. 12. Estimate of the attenuation length (12.1 +/- 4.5 cm) of light response signal in scintillator strip H3. Block E5 is on the side nearest the optical connection for H3, and so the edge of E5 was taken as the 0 cm position. Block E1 ends at 14.2 cm.

6. Conclusions

Much time was spent on understanding the light response by thin, strip scintillators. The amount of light attenuation with distance from the optical connection is non-negligble and must be taken into account if the horizontal and vertical strip arrays are to be used to measure the energy loss of incident ions.

Further consideration of the methods for aligning the thin, strip scintillators is also required. These scintillator strips are prone to crazing, which reduces the light transport efficiency of the strips drastically. In order to extend the time in which these scintillators are usable, the mounting frame design must be changed so as to eliminate all bending forces on the strips, which have been observed to be the leading cause of crazing.

[1] J. Button, R. Polis *et al.*, *Progress in Research*, Cyclotron Institute Texas A&M University (2008-2009), p. V-30.

[2] J.B. Birks, Phys. Rev. **86**, 569 (1952).

[3] J.F. Ziegler, J.P. Biersack, U. Littmark, *The Stopping and Range of Ions in Solids*, (Pergamon Press, New York, 1999).

[4] F.D. Becchetti, C.E. Thorn, M.J. Levine, Nucl. Instrum. Methods **138**, 93 (1976).

[5] H. Bethe, Z. Phys. **76**, 293 (1932).

[6] K. Michaelian, Nucl. Instrum. Methods Phys. Res. **A356**, 297 (1995).

[7] International Commission on Radiation Units and Measurements. *ICRU Report 37, Stopping Powers for Electrons and Positrons*. (1984)

[8] K. Heyde, *Basic Ideas and Concepts in Nuclear Physics: An Introductory Approach*, (Institute of Physics Publishing, Philadelphia, 2004).